Transportation Research Part E 165 (2022) 102867

Contents lists available at ScienceDirect

Transportation Research Part E

journal homepage: www.elsevier.com/locate/tre

An integrated multi-objective model for disaster waste clean-up systems optimization

Cheng Cheng [a], Jia-Wei Lu [b], Rui Zhu [c,d], Zuopeng Xiao [e,*], Alysson M. Costa [f], Russell G. Thompson [g]

[a] School of Transportation, Southeast University, Jiangsu, Nanjing 211189, China
[b] South China Institute of Environmental Sciences, Ministry of Ecology and Environment, Guangzhou 510655, China
[c] Department of Land Surveying and Geo-Informatics, The Hong Kong Polytechnic University, Kowloon, Hong Kong, China
[d] Research Institute for Land and Space, The Hong Kong Polytechnic University, Hong Kong, China
[e] School of Architecture, Harbin Institute of Technology, Shenzhen, China
[f] School of Mathematics and Statistics, The University of Melbourne, VIC 3010, Australia
[g] The Department of Infrastructure Engineering, The University of Melbourne, VIC 3010, Australia

ARTICLE INFO

Keywords:
Disaster waste management
Heavy-duty vehicles
Environmental emission
Mixed integer programming
Optimization
Pareto frontier

ABSTRACT

Post-disaster waste clean-up systems are complex and expensive operations that need to consider multiple stakeholders with different objectives. We propose a mixed-integer programming model that models the waste clean-up operations as a two-echelon system. The model decides on the location of waste processing facilities, the use of demolition resources, and the number and type of vehicles to be assigned to each echelon at each time slot of the planning horizon. The objectives considered in the model include minimizing environmental impacts, economic costs, and total time spent on the operations. Numerical results obtained on a case study based on the '2009 Victoria Black Saturday Bush-fires' case and on synthetically generated instances are used to obtain Pareto frontiers. The research concludes that the three objectives considered are indeed conflictive, and the explicit consideration of each goal can help decision-makers find the best trade-off solutions.

1. Introduction

Waste removal is the first step in the recovery and reconstruction of areas affected by large-scale natural disasters. These debris removal operations are time-consuming, costly, and produce a considerable amount of air pollutants. Quantitative models that are able to simultaneously address these three aspects of the problem can guide decision-makers in the search for the best trade-off solutions during clean-up operations.

Among the three objectives, logistic costs have been the most studied in the literature. They are responsible for a large share of the total cost, and their minimization is generally treated as the foremost goal (Sheu, 2007; Fetter and Rakes, 2012; Lorca et al., 2017; Habib et al., 2019; Hu et al., 2019). A common strategy to reduce logistic costs is the use of *temporary disaster waste management sites* (TDWMSs), where waste can be temporarily stored, sorted, reduced, and processed before final disposal (FEMA, 2007). TDWMSs can help shorten waste collection time by improving the flexibility of operations, facilitating recycling, and reducing waste.

* Corresponding author.
E-mail address: tacxzp@foxmail.com (Z. Xiao).

https://doi.org/10.1016/j.tre.2022.102867
Received 12 April 2021; Received in revised form 30 July 2022; Accepted 7 August 2022
1366-5545/

Table 1
Summary of papers focus on the modeling of disaster waste management systems.

Reference	Research problems Main problem	TDWMSs used	Model Objectives Min cost	Min time	Min emissions	Solution method	Problem size
Özdamar et al., 2014	Open blocked roads	×	×	√	×	Heuristic algorithm	Two road networks with 212 roads and 386 roads, respectively
Pramudita et al., 2014;	Open blocked roads	×	√	×	×	Tabu search *meta*-heuristics	25 to 100 customer nodes
Sahin et al., 2016	Open blocked roads	×	×	√	×	Heuristic algorithm	45 customer nodes
Çelik, Ergun, & Keskinocak, 2015	Open blocked roads	×	×	×	×	Heuristic algorithm	Up to 604 blocked roads
Berktaş, Kara, & Karaşan, 2016	Open blocked roads	×	×	√	×	Heuristic algorithm	Two case studies with 45 and 73 customer nodes, respectively
Onan et al., 2015	Select locations for TDWMSs	√	√	×	×	NSGA-II	45 candidates
Cheng and Thompson, 2016	Select locations for TDWMSs	√	×	×	×	Land suitability analysis	NA
Fetter and Rakes, 2012	Optimize waste clean-up in the recovery stage	√	√	×	×	Robust Programming	49 customer nodes + 8 possible TDWMS locations
Hu and Sheu, 2013	Optimize waste clean-up in the recovery stage	√	√	×	√	Multi-objective linear programming	23 customer nodes + 23 TDWMSs
Takeda et al., 2014	Optimize waste clean-up in the recovery stage	×	√	×	×	Warshall-Floyd algorithm and linear programming	10 customer nodes + 23 TDWMSs
Lorca et al., 2017	Optimize waste clean-up in the recovery stage	√	√	√	√	Mixed Integer programming	12 customer nodes + 14 TDWMSs
Habib et al., 2019	Optimize waste clean-up in the recovery stage without the collection of waste from source to TDWMSs	√	√	×	√	Fuzzy programming	3 TDWMSs + 20 final disposal sites
Hu et al., 2019	Optimize waste clean-up in the recovery stage	×	√	×	×	Mixed Integer programming	30 customer nodes
Mamashli et al., 2021	Optimize waste clean-up in the recovery stage	×	√	×	√	Particle swarm optimization algorithm	13 customer nodes + 18 TWDMSs
Asai et al., 2021	Optimize waste clean-up in the recovery stage	√	×	√	×	Dynamic hauling/ Transportation model	53 customer nodes + 12 TWDMSs
Cheng et al., 2021b	Optimize waste clean-up in the recovery stage	√	√	√	×	Genetic algorithm	125 customer nodes + 10 TDWMSs
The current paper	Optimize waste clean-up in the recovery stage	√	√	√	√	Multi-objective Mixed Integer programming	10 to 500 customer nodes + 8 TDWMSs

Facilities such as TDWMSs divide the waste removal operations into two echelons: the wastes are collected from their origins and transported to a TDWMS, where the waste is stored, processed, and then transported to their final destinations (Alziari et al., 1981; Amato et al., 2020, 2019; Brown and Milke, 2016; Karunasena et al., 2012; Oh and Kang, 2013; Rafee et al., 2008). In this kind of setting, the main decisions are the selection of locations for the TDWMSs, the assignment of vehicles to each of the echelons at each period of the planning horizon and, in the case of large-scale disasters, the scheduling of demolition resources to make waste available for collection (Cheng et al., 2021a).

During operations, a significant amount of air pollutants can be generated at landfills, recycling facilities and, mostly, due to the movement of a large number of heavy-duty vehicles. These emissions depend on the type of vehicles being used and the distances travelled, which are often neglected in the literature (see Section 2). Also, the rapid conclusion of waste operations is also an important goal to consider, as they allow the displaced communities to start returning to their homes and proceed with the recovery of the affected area.

The three objectives are often conflictive and not clearly comparable in terms of their dollar-values. For this reason, we propose a multi-objective approach that is able to provide alternative solutions that can be further evaluated by decision-makers. Our approach relies on a mixed-integer programming model that includes decisions on the location of the TDWMSs, the use of demolition resources, and the number and type of vehicles assigned to each echelon at each timeslot of the planning horizon.

The model proves to be effective to solve problems with up to 500 waste collection points and is used to obtain non-dominated solutions using a normalized normal constraint method (NNCM) (Messac et al., 2003; Sanchis et al., 2008). This approach facilitates the evaluation of solutions' quality in terms of the three different dimensions of the problem, shedding light on urban reverse logistics with a focus on waste clean-up and providing policy-makers with quantitative information that can guide the selection of the best strategies according to the situation at hand.

To analyze and illustrate the effectiveness of the proposed methodology, we present a case study based on the *2009 Black Saturday*

Bush-fires (Brown et al., 2010), which severely affected the State of Victoria, Australia. A number of additional synthetic instances are also generated to better understand the behaviour of the method for problems with different scales.

The remainder of this paper is as follows. A literature review positioning our contributions with respect to the existing research is presented in Section 2. In Section 3, the proposed methodology is described. Section 4 introduces the case study, detailing the data generation process. Section 5 presents the setting and the results of the computational experiments. Section 6 ends this paper with an overview of the managerial insights that can be obtained and some concluding remarks.

2. Literature review

Waste clean-up operations can be seen as a reverse logistic problem (Hu and Sheu, 2013), in which commodities (waste) must be collected at consumer locations, moved through logistic facilities, and transported to their final destinations. The amount of waste generated through disasters can exceed multiple times the yearly amount generated in municipal waste collection, giving rise to large-scale operations (Zhang et al., 2019; Lu et al., 2015, 2018). In large-scale disasters, the demolition of destroyed buildings and the selection of locations for TDWMSs further increase the complexity of the problem (Cheng et al., 2021a). The following sections review the related literature. Table 1 summarizes research problems, objectives, solution methods, and problem sizes considered in the literature. The most important contributions are summarized in the remainder of this section.

2.1. Disaster waste clean-up problems

Several studies aim at examining how to open blocked roads and ensure that vital activities such as evacuation, rescue, and relief can proceed in the response stage of disaster management (Özdamar et al., 2014; Pramudita et al., 2014; Çelik et al., 2015, Sahin et al., 2016). Other studies are interested in seeking optimal routes either for relief or waste clean-up operations (Hu and Sheu, 2013; Takeda et al., 2014; Lorca et al., 2017). When the focus is on waste clean-up, researchers consider the necessity of designing complex operation structures. This is usually done with the use of intermediate facilities, generating an extensive literature on the location of TDWMSs (Cheng and Thompson, 2016; Kim et al., 2014; Fetter and Rakes, 2012; Habib et al., 2019; Hu et al., 2019, Onan et al., 2015).

2.2. Optimization objectives and algorithms

Regarding the optimization objectives, different objectives are considered subject to research purposes. Minimizing total operation cost was firstly taken as the foremost objective in relevant studies (Fetter and Rakes, 2012; Hu and Sheu, 2013; Onan et al., 2015; Lorca et al., 2017; Habib et al., 2019; Hu et al., 2019). These costs include all fees paid for waste collection and transportation, disposal and storage reduction operations, and project management. The time spent on waste clean-up has been recognized as another important objective, as it can directly affect the recovery process of disaster-affected areas (Brown et al., 2011a; Lorca et al., 2017).

Waste removal by heavy-duty vehicles inevitably exerts critical environmental footprints such as CO_2, SO_x, NO_x, and PM. These emissions have substantial impacts on human health and the living environment. In line with the rising environmental concerns, a growing number of studies included environmental emissions in their optimization objectives (Hu and Sheu, 2013; Lorca et al., 2017; Habib et al., 2019).

2.3. Solution method

Considering the complexity of the post-disaster waste clean-up system, some models attempted to deal with multiple objectives. Usually, the multi-objective problems are solved by normalizing considered objectives and minimizing the weighted sum of all objectives (Lorca et al., 2017; Hu and Sheu, 2013) or by using heuristic algorithms such as NSGA-II (Onan et al., 2015; Zhong et al., 2020; Qiu et al., 2021). However, converting multiple objectives into a single objective can only generate a single solution per calculation, while heuristics algorithms cannot guarantee the quality of solutions.

2.4. Problem size

The research aimed to open blocked roads using the number of nodes needed to reach (Pramudita et al., 2014; Sahin et al., 2016; Berktaş, Kara, & Karaşan, 2016) or the number of roads in the network (Özdamar et al., 2014; Çelik, Ergun, & Keskinocak, 2015) to represent the scale of the problem. The largest scale of the problem researched includes 100 customer nodes (Pramudita et al., 2014) and 604 roads in the network (Çelik, Ergun, & Keskinocak, 2015). Papers focused on the recovery stage of disaster waste clean-up normally used the number of customer nodes and the number of TDWMSs in the system to measure problem size. In these studies, problem sizes were generally small, with the largest problem involving 125 customer nodes and 10 TDWMSs (Cheng et al., 2021b).

2.5. Discussion

As mentioned early, one of the main gaps in the literature is that current studies have not managed to explicitly consider different optimization objectives in the design of waste clean-up systems. Namely, the environmental objectives have not been handled together with economic or efficiency objectives. Regarding solution methods, heuristics algorithms are most frequently used (Özdamar et al., 2014; Pramudita et al., 2014; Çelik et al., 2015; Onan et al., 2015; Sahin et al., 2016, Berktaş et al., 2016). A few studies used mixed-

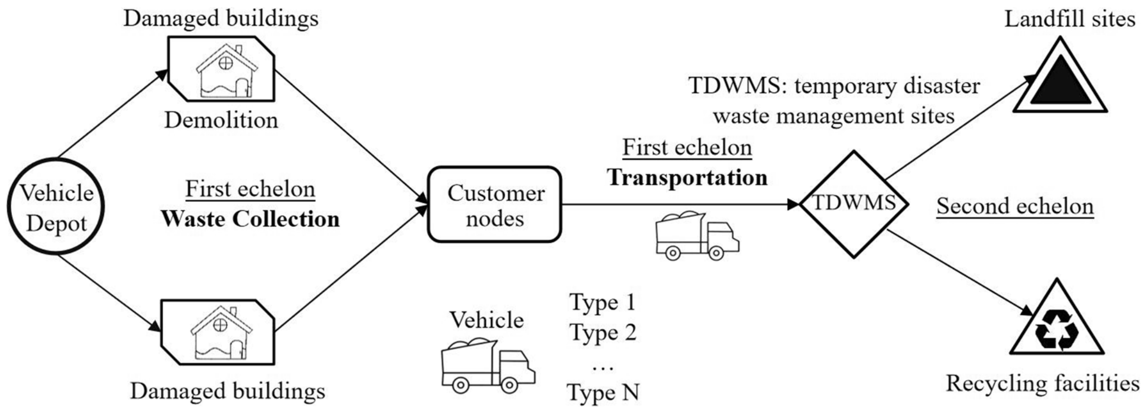

Fig. 1. Two-echelon disaster waste clean-up system structure.

integer programming and resorted to black-box solvers to obtain optimal solutions for the models proposed (Hu and Sheu, 2013; Hu et al., 2019).

To bridge this research gap, the post-disaster waste clean-up system model in this study explicitly considers the total environmental emission, the total cost, and the total time required to complete the waste clean-up. The main tasks of the model are to decide on TDWMS locations and the movements of heavy-duty vehicles from collection points to intermediate facilities and from there to final disposal facilities.

This study proposes a mixed-integer programming model that is used in the process of obtaining Pareto frontiers. Methods to generate Pareto solutions include the physical programming method, the typical boundary intersection method, the normal constraint method, the weighted sum method, the compromise programming method, and NNCM. This paper applies the NNCM proposed by Messac et al. (2003). Small and large-scale instances (25 to 500 customer nodes) are used to test the methodology.

3. Problem description and mathematical model

3.1. Problem description

We consider the problem of designing and managing a two-echelon waste clean-up system. The location of the temporary waste processing sites (TDWMS) is the central decision in the problem as they define the frontier between the two echelons of the problem. The problem is depicted in Fig. 1 and can be described in four stages: demolition, collection, processing, and transportation. In the first echelon, demolition resources are used to generate the waste to be collected at the *customer nodes*. The order of demolition is crucial as it defines the nodes available for collection at each period of the planning horizon. Nodes with available waste are then visited by collection trucks, and the waste is transported to the TDWMSs where waste is stored and processed. Finally, the processed waste is transported to its final destinations, either landfills or recycling facilities by vehicles in the second echelon.

The following assumptions are made:

- All recyclable waste is regarded as one category, which will be sent to the recycling facilities after separation and processing at TDWMSs;
- The waste clean-up planning horizon is discretized in units of half a month (15 days);
- The number and types of each available vehicle are known a priori. Different vehicles may have different capacities.
- The quantity of pollutants emitted during a trip depends on the vehicle type, load and distance travelled.
- A vehicle travels directly from customer nodes to TDWMSs and to the final disposal sites (no routing).
- Demolition operations are continuous, and the amount of waste generated at each period depends on the demolition speed which is assumed to be an input parameter.
- Candidate locations for TDWMS are known, as well as the costs to implement a processing facility at each location.

Given these characteristics, the problem consists in deciding the location of the TDWMS and, for each period of the planning horizon: the order in which the buildings are demolished to generate the waste to be collected, the quantity and types of vehicles assigned to each echelon of the problem, and the flow of waste in each echelon.

3.2. Mathematical model

A graph $G = (N, A)$ is defined to describe the problem. The set of nodes N contains all relevant locations in the problem, $N = C \cup J \cup L \cup R$, in which $C = \{1, 2, \ldots, n\}$ is the set of customer nodes, $J = \{n+1, n+2, \ldots, n+m\}$ is the set of TDWMS, $L = \{n+m+1, n+m+2, \ldots, n+m+l\}$ denotes landfill sites, and $R = \{n+m+l+1, n+m+l+2, \ldots, n+m+l+r\}$ denotes the recycling facilities. The set

A, in turn, contains the transportation links between the nodes in N, $A = \{ (i, j), \forall i, j \in N\}$.

The input parameters of the model, as described in Section 4, are as follows:

Input parameters:

d_{ij}: Distance between node i and node j, $i, j \in$ N (Unit: Km).

D_i: Demand of customer node i, $i \in$ C (Unit: tonne).

M: Demolition capacity (Unit: tonne/timeslot).

η: Disaster waste recycling rate.

W: Set of waste clean-up period (Unit: timeslot = 15 days).

K: Set of vehicle types.

f_k: Fixed cost of selecting a vehicle of type k, $k \in$ K.

F: Maximum fixed cost can be spent on vehicles.

V_k^0: Maximum number of type $k \in$ K vehicle that is available.

V^T: Number of vehicles in the fleet.

Q_k: Capacity of vehicle type $k \in$ K.

t_k^1: Number of trips a type k $\in$ K vehicle can conduct in the collection stage in a time slot.

t_k^2: Number of trips a type k $\in$ K vehicle can conduct in the transportation stage in a time slot.

S_j: Capacity of TDWMS j $\in$ J (Unit: tonne).

C_k^{VOC}: Operation cost of vehicle type k $\in$ K (Unit: AUD/Km).

C_k^{VOT}: Time cost of vehicle type k $\in$ K (Unit: AUD/Km).

C_k^{EC}: Environmental cost of vehicle type k $\in$ K (Unit: AUD/Km).

C_k^{SC}: Social cost of vehicle type k $\in$ K (Unit: AUD/Km).

c^S: Waste storage cost in TDWMSs (Unit: AUD/tonne).

c^L: Waste landfill cost (Unit: AUD/tonne).

c^R: Waste recycling cost (Unit: AUD/tonne).

E: Set of environmental emissions considered in the problem, E = {CO2, Sox, Nox, PM}.

p_k^e: e $\in$ E emission of vehicle type k $\in$ K (Unit: Kg/(tonne · Km)).

p^{e_s}: e $\in$ E emission from waste storage at TDWMSs (Unit: Kg/tonne).

p^{e_L}: e $\in$ E emission from waste landfill (Unit: Kg/tonne).

p^{e_R}: e $\in$ E emission from waste recycling facilities (Unit: Kg/tonne).

The set of decision variables is divided into main and auxiliary decisions, as follows:

Main decision variables:

$x_{ijk\omega}$: Amount of waste collected from customer node $i \in$ C to TDWMSs $j \in$ J by vehicle type $k \in$ K in time slot $w \in$ W (Unit: tonne).

$y_{jlk\omega}$: Amount of waste transported from TDWMSs $j \in$ J to landfill $l \in$ L by vehicle type $k \in$ K in time slot $w \in$ W (Unit: tonne).

$z_{jrk\omega}$: Amount of waste transport from TDWMSs $j \in$ J to recycling facilities $r \in$ R by vehicle type $k \in$ K in time slot $w \in$ W (Unit: tonne).

w_j : Binary variable equal to 1 if TDWMS $j \in$ J is selected, 0 otherwise.

$s_{j\omega}$: Amount of waste stored in a TDWMS $j \in$ J at the end of time slot $w \in$ W (Unit: tonne, $s_{j0} = 0, \forall j \in$ J).

V_k : Number of vehicle type $k \in$ K used in the system.

$v_{k\omega}^1$: Number of vehicle type k $\in$ K involved in the waste collection (first echelon) in time slot $w \in$ W.

$v_{k\omega}^2$: Number of vehicle type k $\in$ K involved in waste transportation (second echelon) in time slot $w \in$ W.

Auxiliary variables:

γ_ω: Binary variable equal to 1 if all the waste is cleaned at the end of time slot $w \in$ W, 0 otherwise.

G_{iw}: Amount of waste produced at customer node $i \in$ C in time slot $w \in$ W (Unit: tonne).

$g_{i\omega}$: Amount of available waste accumulated at customer node $i \in$ C at the end of a time slot $w \in$ W (Unit: tonne, gw = 0).

C^T: Total cost of waste clean-up (Unit: AUD).

C_ω^{VOC}: Operation cost of the system in time slot $w \in$ W (Unit: AUD).

C_ω^{VOT}: Time cost of the system in time slot $w \in$ W (Unit: AUD).

C_ω^{EC}: Environmental cost of the system in time slot $w \in$ W (Unit: AUD).

C_ω^{SC}: Social cost of the system in time slot $w \in$ W (Unit: AUD).

C_ω^s: Waste storage cost in TDWMSs in time slot w $\in$ W (Unit: AUD).

C_ω^L: Waste landfill costs in time slot $w \in$ W (Unit: AUD).

C_ω^R: Waste recycling cost in time slot $w \in$ W (Unit: AUD).

P_T^e: Total e $\in$ E emission from the whole waste clean-up system (Unit: Kg).

P_ω^{1e}: e $\in$ E emission from waste collection stage in time slot $w \in$ W (Unit: Kg).

P_ω^{2e}: e $\in$ E emission from waste transportation stage in time slot $w \in$ W (Unit: Kg).

P_ω^{se}: e $\in$ E emission from waste storage in TDWMSs in time slot $w \in$ W (Unit: Kg).

P_ω^{Le}: e $\in$ E emission from waste landfill in time slot $w \in$ W (Unit: Kg).

P^{Re}_{ω}: e ∈ E emission from waste recycling in time slot $w \in$ W (Unit: Kg).

The three objectives of the problem are as below:

$$min\sum_{e\in E}P^{e}_{T} \tag{1}$$

$$minC^{T} \tag{2}$$

$$min|W|-\sum_{w\in W}\gamma_{w}+1 \tag{3}$$

Objective (1) concerns the minimization of total emissions. Objective (2) aims to minimize the total cost of logistic operations, while objective (3) aims to minimize the total time required to finish the clean-up operations.

The logistic constraints below ensure that the capacities of vehicles and processing sites are respected and that all demand is collected within the measured time horizon.

$$\sum_{k\in K}V_{k}f_{k}\leq F, \tag{4}$$

$$\sum_{i\in C}G_{i\omega}\leq M,\forall\omega\in W \tag{5}$$

$$G_{i\omega}\leq D_{i},\forall i\in C,\omega\in W \tag{6}$$

$$\sum_{\omega\in W}G_{i\omega}=D_{i},\forall i\in C \tag{7}$$

$$\sum_{j\in J}\sum_{k\in K}x_{ijk\omega}+g_{i\omega}=G_{i\omega}+g_{i\omega-1},\forall i\in C,\omega\in W \tag{8}$$

$$(1-\eta)\sum_{i\in C}\sum_{k\in K}x_{ijk\omega}+s_{j\omega-1}-s_{j\omega}=\sum_{l\in L}\sum_{k\in K}y_{jlk\omega},\forall j\in J,\omega\in W \tag{9}$$

$$\eta(\sum_{i\in C}\sum_{k\in K}x_{ijk\omega}+s_{j\omega-1}-s_{j\omega})=\sum_{r\in R}\sum_{k\in K}z_{jrk\omega},\forall j\in J,\omega\in W \tag{10}$$

$$0\leq s_{j\omega}\leq S_{j}w_{j},\forall j\in J,\omega\in W \tag{11}$$

$$\sum_{i\in C}\sum_{j\in J}x_{ijk\omega}\leq t^{1}_{k}\,v^{1}_{k\omega}Q_{\mathrm{k}}\,,\forall k\in K,\omega\in W \tag{12}$$

$$\sum_{l\in L}\sum_{j\in J}y_{jlk\omega}+\sum_{r\in R}\sum_{j\in J}z_{jrk\omega}\leq t^{2}_{k}\,v^{2}_{k\omega}Q_{\mathrm{k}}\,,\forall k\in K,\omega\in W \tag{13}$$

$$\sum_{j\in J}\sum_{k\in K}\sum_{\omega\in w}x_{ijk\omega}=D_{i},\forall i\in C \tag{14}$$

$$\sum_{i\in C}\sum_{k\in K}\sum_{\omega\in W}x_{ijk\omega}=\sum_{l\in L}\sum_{k\in K}\sum_{\omega\in W}y_{jlk\omega}+\sum_{r\in R}\sum_{k\in K}\sum_{\omega\in W}z_{jrk\omega},\forall j\in J \tag{15}$$

$$\sum_{k\in K}V_{k}\leq V^{T}, \tag{16}$$

$$V_{k}\ \leq V^{0}_{k},\forall k\in K \tag{17}$$

$$v^{1}_{k\omega}+v^{2}_{k\omega}\leq V_{k}\,,\forall k\in K,\omega\in W \tag{18}$$

$$g_{|W|}=0, \tag{19}$$

$$s_{j|W|}=0,\forall j\in J \tag{20}$$

$$(1-\eta)\sum_{i\in C}\sum_{k\in K}\sum_{\omega\in W}x_{ijk\omega}=\sum_{l\in L}\sum_{k\in K}\sum_{\omega\in W}y_{jlk\omega},\forall j\in J \tag{21}$$

$$\eta\sum_{i\in C}\sum_{k\in K}\sum_{\omega\in W}x_{ijk\omega} = \sum_{r\in R}\sum_{k\in K}\sum_{\omega\in W}z_{jrk\omega}, \forall j \in J \tag{22}$$

$$\gamma_w \leq 1 - \frac{D_i - \Sigma_{\omega'=1}^{\omega}G_{i\omega'} + g_{i\omega}}{D_i}, \forall i \in C, \omega \in W \tag{23}$$

$$\gamma_w \leq 1 - \frac{s_{j\omega}}{S_j}, \forall j \in J, \omega \in W \tag{24}$$

Constraints (4) ensure the maximum fixed cost of vehicles is not exceeded. Constraints (5) guarantee that the total amount of waste generated in a time slot is no more than the demolition capacity. Constraints (6) limit the waste produced in a customer node in each time slot to the total demand of the customer node. Constraints (7) ensure that all customer nodes are properly processed by demolition operations, making their waste available for collection. Constraints (8) are waste flow balance constraints at each customer node and ensure that only available waste can be collected at each time slot. Constraints (9) and (10) are flow balance constraints in TDWMSs for landfill waste and recyclable waste, respectively. They measure the waste inventory at each TDWMS and, along with Constraints (11) ensure that a TDWMS can only be used if it is open and that the stored waste at each time slot must respect the site capacity. Constraints (12) and (13) are vehicle capacity constraints in the waste collection and transportation stages, respectively. These constraints approximate the management of vehicle capacities using a proxy given by the total number of trips that can be conducted at each time slot, at each echelon, given the characteristics of the selected fleet.

Constraints (14) force all waste generated by demolition at each customer to be collected. Constraints (15) ensure that all waste sent to each TDWMS should be transported to final disposal sites (landfills or recycling facilities). Constraints (16) ensure that the total number of vehicles used is bounded by the existing fleet. Constraints (17) are the counterpart of Constraints (16) for each vehicle type. Constraints (18) assign the available vehicles to the two echelons of the problem. Constraints (19) and (20) ensure all the waste has been cleaned at the end of the planning horizon. Constraints (21) and (22) guarantee that all non-recyclable waste ends in landfills and all recyclable waste ends in recycling facilities. Constraints (23) and (24) guarantee the correct meaning of artificial variables γw, $w \in W$, that is, γw can be set at 1 only if all the waste is cleaned at the end of time slot w.

The additional constraints below are used to compute the environmental emissions generated in waste collection, transportation, storage, landfill, and recycling in every time slot for each environmental factor.

$$p_{\omega}^{1e} = \sum_{i\in C}\sum_{j\in J}\sum_{k\in K}\left(x_{ijk\omega}p_k^e d_{ij}\right), \forall e \in E, \omega \in W \tag{25}$$

$$p_{\omega}^{2e} = \sum_{l\in L}\sum_{j\in J}\sum_{k\in K}\left(y_{jlk\omega}p_k^e d_{jl}\right) + \sum_{r\in R}\sum_{j\in J}\sum_{k\in K}\left(z_{jrk\omega}p_k^e d_{jr}\right), \forall e \in E, \omega \in W \tag{26}$$

$$p_{\omega}^{se} = p^{e-s}\sum_{j\in J}s_{j\omega}, \forall e \in E, \omega \in W \tag{27}$$

$$p_{\omega}^{Le} = p^{e-L}\sum_{l\in L}\sum_{j\in J}\sum_{k\in K}y_{jlk\omega}, \forall e \in E, \omega \in W \tag{28}$$

$$p_{\omega}^{Re} = p^{e-R}\sum_{r\in R}\sum_{j\in J}\sum_{k\in K}z_{jrk\omega}, \forall e \in E, \omega \in W \tag{29}$$

$$p_T^e = \sum_{\omega\in W}\left(p_{\omega}^{1e} + p_{\omega}^{2e} + p_{\omega}^{se} + p_{\omega}^{Le} + p_{\omega}^{Re}\right), \forall e \in E \tag{30}$$

$$C_{\omega}^{VOC} = \sum_{i\in C}\sum_{j\in J}\sum_{k\in K}\left(x_{ijk\omega}c_k^{VOC}d_{ij}\right) + \sum_{l\in L}\sum_{j\in J}\sum_{k\in K}\left(y_{jlk\omega}c_k^{VOC}d_{jl}\right) + \sum_{r\in R}\sum_{j\in J}\sum_{k\in K}\left(z_{jrk\omega}c_k^{VOC}d_{jr}\right), \forall \omega \in W \tag{31}$$

$$C_{\omega}^{VOT} = \sum_{i\in C}\sum_{j\in J}\sum_{k\in K}\left(x_{ijk\omega}c_k^{VOT}d_{ij}\right) + \sum_{l\in L}\sum_{j\in J}\sum_{k\in K}\left(y_{jlk\omega}c_k^{VOT}d_{jl}\right) + \sum_{r\in R}\sum_{j\in J}\sum_{k\in K}\left(z_{jrk\omega}c_k^{VOT}d_{jr}\right), \forall \omega \in W \tag{32}$$

$$C_{\omega}^{EC} = \sum_{i\in C}\sum_{j\in J}\sum_{k\in K}\left(x_{ijk\omega}c_k^{EC}d_{ij}\right) + \sum_{l\in L}\sum_{j\in J}\sum_{k\in K}\left(y_{jlk\omega}c_k^{EC}d_{jl}\right) + \sum_{r\in R}\sum_{j\in J}\sum_{k\in K}\left(z_{jrk\omega}c_k^{EC}d_{jr}\right), \forall \omega \in W \tag{33}$$

$$C_{\omega}^{SC} = \sum_{i\in C}\sum_{j\in J}\sum_{k\in K}\left(x_{ijk\omega}c_k^{SC}d_{ij}\right) + \sum_{l\in L}\sum_{j\in J}\sum_{k\in K}\left(y_{jlk\omega}c_k^{SC}d_{jl}\right) + \sum_{r\in R}\sum_{j\in J}\sum_{k\in K}\left(z_{jrk\omega}c_k^{SC}d_{jr}\right), \forall \omega \in W \tag{34}$$

$$C_{\omega}^{s} = \sum_{j\in J}s_{j\omega}C^{s}, \forall \omega \in W \tag{35}$$

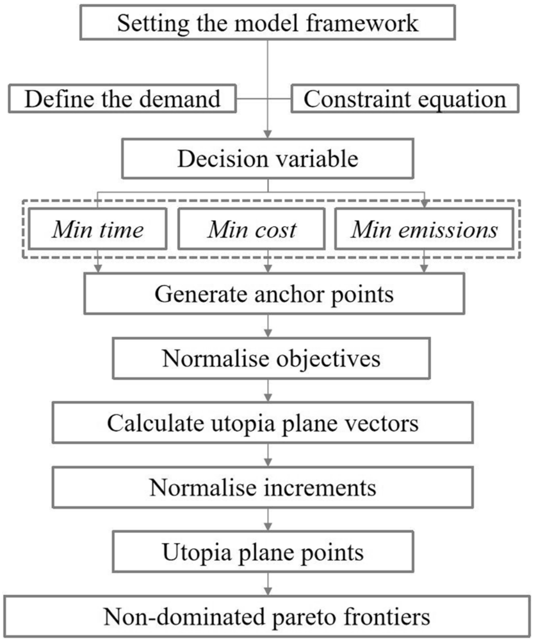

Fig. 2. Modeling flow.

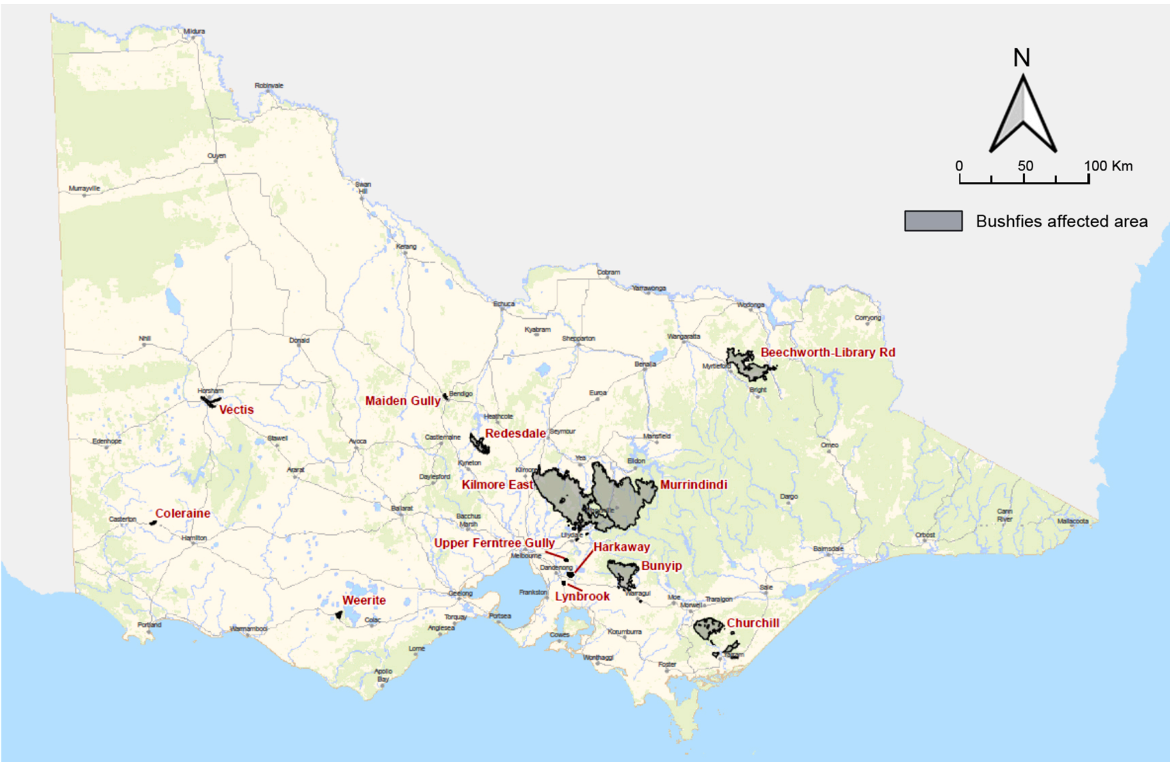

Fig. 3. Spatial distribution of significant fires of the 2009 Black Saturday Bush-fires.

$$C^L_\omega = \sum_{l\in L}\sum_{j\in J}\sum_{k\in K} y_{jlk\omega} C^L, \forall \omega \in W \tag{36}$$

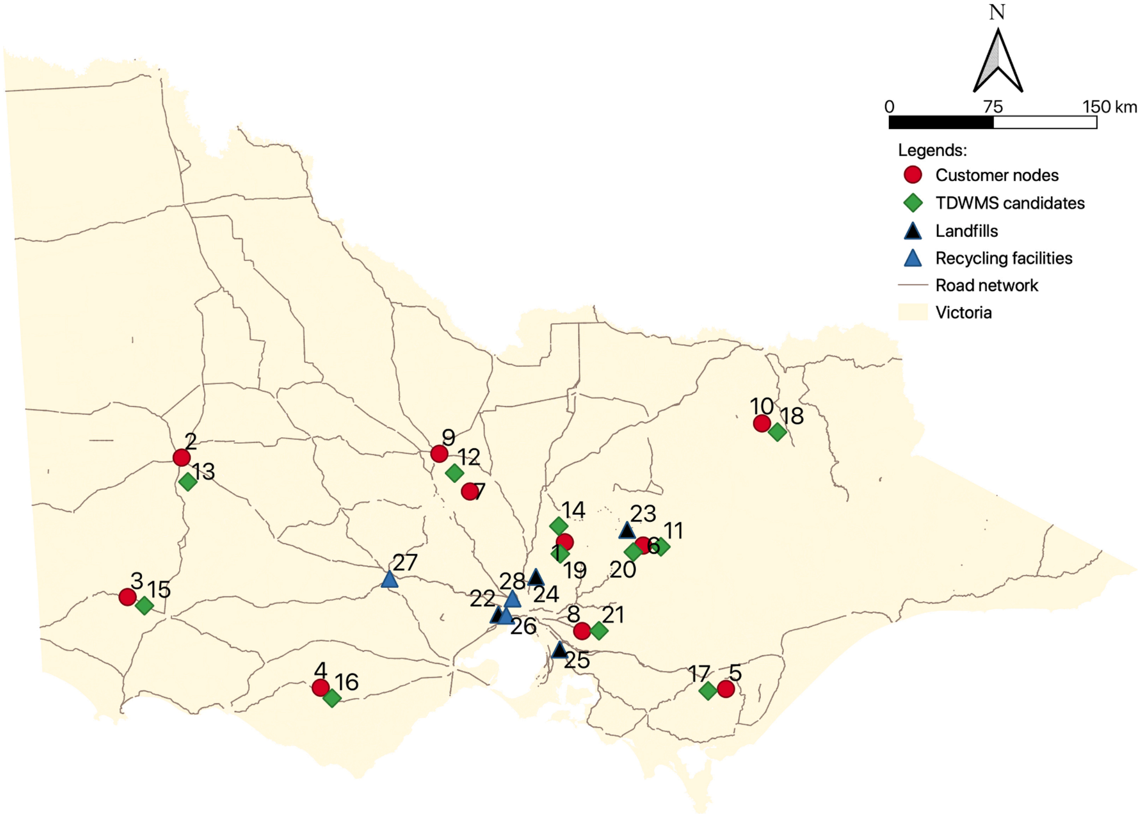

Fig. 4. The nodes are distributed in the study area.

$$C_{\omega}^{R} = \sum_{r\in R}\sum_{j\in J}\sum_{k\in K} z_{jrk\omega} C^{R}, \forall \omega \in W \tag{37}$$

$$C^{T} = \sum_{\omega\in W}\left(C_{\omega}^{VOC} + C_{\omega}^{VOT} + C_{\omega}^{EC} + C_{\omega}^{SC} + C_{\omega}^{s} + C_{\omega}^{L} + C_{\omega}^{R}\right) + \sum_{k\in K} V_k f_k \tag{38}$$

Constraints (25) to (29) compute the emissions according to the vehicle trips. Constraints (30) compute total environmental cost, and Constraints (35) to (37) are used to compute the environmental costs in each time slot according to different components of the system, that is, waste storage cost, waste landfill cost, and waste recycling cost, respectively. Constraints (38) give the total cost of the system.

3.3. Methodology for generating Pareto curves

After modeling the objectives respectively, the model attempts to normalize the objectives to define the Utopia point and generate the Pareto frontier. To generate Pareto points, we run the optimization for J times by minimizing the total time objective considering the additional constraints (A7) to (A9) in Appendix A for each run j. We applied the Pareto filter to produce a subset of the Pareto points (Messac et al., 2003) in which all dominated points are removed. The modeling flow is summarized in Fig. 2.

4. Case study

4.1. Case study area

The Black Saturday bushfires were a series of bushfires that ignited or burned across the Australian State of Victoria on and around Saturday, 7 February 2009. They were one of the worst bushfires disasters in Australian history. It has influenced several millions of the population in the State, across Australia, and internationally. 173 people were killed in 78 communities, over 430,000 ha of land, and 2000 properties were destroyed (Brown et al., 2010). Fig. 3 shows the significant fires observed in the Black Saturday Bush fires.

Table 2
Data related to customer nodes.

No. of nodes	Location	No. of destroyed buildings	No. of demolished buildings	Damaged land (ha)	Waste from demolished Buildings (tonnes)	Waste from damaged land (tonnes)	Total (tonnes)
1	Kilmore East	1,242	1,812	125,383	308,221.2	33,3371	641,592
2	Horsham(Vectis & Haven)	13	19	2,346	3,232	6,238	9,470
3	Coleraine	1	1	713	170	1,896	2,066
4	Pomborneit-Weerite	0	0	1,008	0	1,896	2,680
5	Churchill	145	212	25,861	36,061	68,760	104,821
6	Murrindindi	538	785	168,542	133,529	448,123	581,652
7	Redesdale	14	20	7,086	3,402	18,840	22,242
8	Narre Warren and Upper Ferntree Gully	7	10	163	1,701	433	2,134
9	Bendigo	58	85	341	14,459	907	15,365
10	Beechworth-Mudgegonga	38	55	33,577	9,356	89,275	98,631
Total		2,056	3,000	365,020	510,130	970,524	1,480,654

Table 3
Summary of data related to vehicles.

Vehicle type	Unit	Type 1	Type 2	Type 3	Type 4
Vehicle capacity	*tonnes*	5	10	15	20
Vehicle quantity		300	200	50	50
Fixed cost	*AUD/vehicle*	2,342	6,032	9,416	17,804
Vehicle travel capacity in stage 1	*trip/timeslot*	30	30	30	30
Vehicle travel capacity in stage 2	*trip/timeslot*	15	15	15	15
Vehicle operation cost (VOC)	*AUD/(t·Km)*	0.566	0.164	0.394	0.254
Value of time (VOT)	*AUD/(t·Km)*	0.113	0.056	0.038	0.029
Environmental cost (EC)	*AUD/(t·Km)*	0.47	0.151	0.345	0.24
Social cost (SC)	*AUD/(t·Km)*	0.491	0.466	0.311	0.356
CO_2 emission	*Kg/(t·Km)*	8.59×10^{-2}	7.82×10^{-2}	7.20×10^{-2}	6.32×10^{-2}
SO_x emission	*Kg/(t·Km)*	7.00×10^{-4}	5.72×10^{-4}	5.04×10^{-4}	4.55×10^{-4}
NO_x emission	*Kg/(t·Km)*	1.19×10^{-3}	9.03×10^{-4}	7.78×10^{-4}	7.04×10^{-4}
PM emission	*Kg/(t·Km)*	1.13×10^{-4}	1.01×10^{-4}	9.12×10^{-5}	8.08×10^{-5}

Note: 1 AUD = 0.79 USD in the year 2009.

4.2. Data collection and organization

4.2.1. Nodes

The nodes involved in the problem are customer nodes, TDWMSs candidates, landfills, and recycling facilities. Fig. 4 presents the spatial locations of the nodes identified in the study area. In total, there are 10 customer nodes, 11 TDWMSs candidates, 4 landfills, and 3 recycling facilities in the case study.

Customer nodes are derived from where houses were destroyed or land damaged. All damage information was summarized on the official website of the Country Fire Authority.[1] The demand of each customer node (*Di*) is calculated using Equation (39).

$$D_i = \alpha N_i + \beta A_i \tag{39}$$

Where D_i is the demand of a customer node $i \in C$; α refers to the average waste generation rate for each demolished house (170.1 tonnes/house), and β is the average waste generation rate of damaged land (265.9 tonnes/km^2) (Rawtec, 2015); N_i and *Ai* are the number of destroyed houses and the area of damaged land in customer node $i \in C$, respectively.

Table 2 shows the destroyed buildings and damaged areas in each customer node. The total number of the destroyed building was about 2000. However, there were 3,000 buildings demolished (Brown et al., 2010). Thus, we assume that the number of demolished buildings is directly proportional to the number of destroyed buildings.

TDWMS candidates are selected respecting the method developed by Cheng and Thompson (2016). The capacity of each candidate (*Sj*) is estimated by Equation (40) (Tabata et al., 2017), where a_j is the land area of a TDWMS $j \in J$, d is the volume-weight of disaster waste ($m^3/tonne$), and H is the height for stacking the disaster waste (m).

$S_j = (a_j \times H)/d$ (40).

In the actual post-disaster waste clean-up system, all these wastes were classified as a single category named "bushfire waste" that was transported to three landfills ultimately (Brown et al., 2010). Although a small part of the waste, such as concrete and metal, was

[1] https://www.cfa.vic.gov.au/about/black-Saturday/.

Table 4
Cost and environmental emission rate of TDWMS and waste final disposal.

	Cost (AUD/t)	CO2 emission (Kg/t)	SO_x emission (Kg/t)	NO_x emission (Kg/t)	PM emission (Kg/t)
Operation in TDWMS	15	4.96	4.60×10^{-4}	2.04×10^{-3}	1.23×10^{-20}
Landfill	0	2.29	6.20×10^{-4}	4.91×10^{-1}	6.75×10^{-4}
Recycling	−44	−1.61	-7.43×10^{-4}	-9.64×10^{-4}	-1.57×10^{-14}

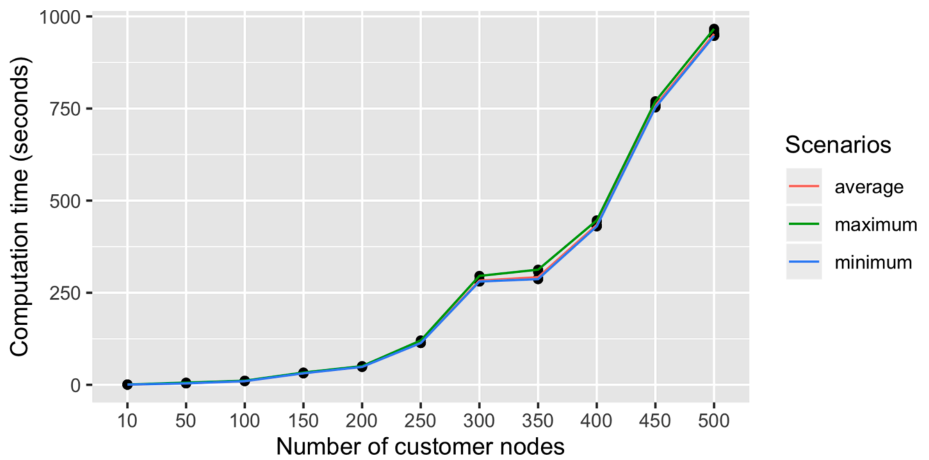

Fig. 5. Computation time of instances with different numbers of customer nodes.

recycled, there was no information about the recycling facilities in the existing waste clean-up system. Thus, three extensive recycling facilities close to the disaster-affected area are considered. The capacity of these facilities is assumed to be big enough to handle all waste generated from the bushfires. The recycling rate is 50 % because the potential recyclable waste can reach 53 % after bushfires (County of San Diego, 2005). The distance between each pair of nodes is calculated using Dijkstra's algorithm, which provides the shortest paths between origin and destination in the platform of ArcGIS software.

4.2.2. Vehicles

The clean-up used 600 vehicles in the Black Saturday Bush-fires waste clean-up operations (Brown et al., 2010). Four vehicle types used in this study have characteristics described in Table 3. Each vehicle type has specific capacities, fixed cost, vehicle operation cost (VOC), the value of time (VOT), environmental cost (EC), and social cost (SC) (Yang et al., 2016). The CO_2 emissions, SO_x emissions, NO_x emissions, and PM emissions for each type of vehicle are also different (Tabata et al., 2017). Vehicle travel capacity defines the number of trips made by each vehicle in each time slot, which is estimated based on the average distance between nodes, the speed of vehicles, and the load and unload time required. The fixed cost, VOC, VOT, EC, and SC of each type of vehicle are obtained from Yang et al. (2016) (Table 3). The total environmental emissions are calculated using the life cycle assessment method derived from Tabata et al. (2017). Namely, the total emission value includes emissions from waste collection and transportation, temporary storage and process in TDWMSs, and final disposal in landfills or recycling facilities.

4.2.3. TDWMS and final disposal

Table 4 provides the cost and environmental emission rate for waste operation in TDWMS, waste recycling, and waste landfill, respectively. The TDWMS operation cost is drawn from EPA (2016). Waste landfill cost is assumed to be zero since the landfill operators are most likely to waive the levy for the waste generated in a disaster. The landfill levy fee was waived to dispose of waste generated from the 2009 Black Saturday bushfires (Brown et al., 2011b). The recycling profit is derived from ACT RECYCLING (2016), assuming that most of the recyclable waste is masonry as it contributes more than 60 % of the total waste generated in a large-scale bushfire (Rawtec, 2015). The environmental emission data is obtained from Tabata et al. (2017).

5. Results analysis and discussion

5.1. Instance generation

We generated artificial instances from small to large scales to test the model's performance. Based on the definition in Syrichas and Crispin (2017). Instances with 250 to 500 nodes are large instances. Therefore, we generated instances with 10 to 500 customer nodes. Each instance was repeated 10 times. In the artificial instances, the location of the customer nodes, TDWMSs, and final disposal

Table 5
Results comparison of different scenarios.

Objective	Min total cost (AUD)		Min total environmental emission (Kg)		Min total time (time slot)	
	Scenario 1	Scenario 2	Scenario 1	Scenario 2	Scenario 1	Scenario 2
Total cost (AUD)	1.17×10^8	2.28×10^8	1.27×10^8	2.29×10^8	5.56×10^8	8.94×10^8
Total environmental emission (Kg)	1.76×10^7	1.27×10^8	1.60×10^7	1.27×10^8	4.96×10^7	1.62×10^8
Total time (time slot)	24	60	24	60	17	50
No. of vehicles required	459	496	400	600	600	600
Type1	0	496	0	600	0	600
Type2	300	0	0	0	244	0
Type3	0	0	200	0	156	0
Type4	159	0	200	0	200	0

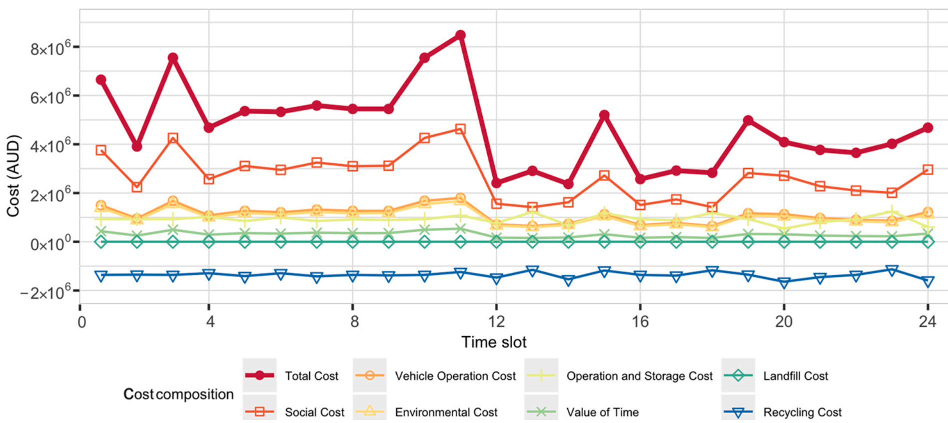

Fig. 6. Detailed cost composition in each time slot when minimizing total cost.

facilities are generated randomly in a rectangle similar to the case study area (400 km × 200 km). The maximum clean-up time is 36 slots for instances with more than 350 customer nodes. The rest of the parameters are the same as the case study.

5.2. Performance of the model

The model is solved using a Gurobi 8.1 solver in an Intel Core i5 @ 2.3 GHz machine with 8 GB RAM. The stopping criterion is a gap smaller than 0.01 %, guaranteeing the near optimal solution. The computation time for each instance is shown in Fig. 5. It illustrates that the model can solve large-scale problems within acceptable computational times for such a planning problem.

5.3. Scenario analysis

We compare the results in two different scenarios. The first scenario respects the model we presented in Section 3, in which different types of vehicles are considered. We create a baseline scenario in the second one assuming only one type of vehicle is used. For example, in the 2004 Marmara Earthquake in Turkey, three-axle trucks with a capacity of 10 tonnes were used in the clean-up process (Baycan, 2004). Thus, we assume that only Type 1 vehicles are used in the clean-up in the second scenario. To allow the model to generate feasible solutions in this scenario, we relaxed the constrain for the maximum clean-up time, which allowed the clean-up to finish in 60 time slots instead of 24 time slots in the original model.

Table 5 compares the results of the two scenarios with three different objectives. It indicates that using Type 2, Type 3, and Type 4 vehicles can save about 50 % of the total cost when the objective is to minimize total cost. When we minimize the total environmental emission, the emission decreases by around 87 % in the first scenario compared to the baseline. Furthermore, the total clean-up time can be reduced by two-thirds if Type 2, Type 3, and Type 4 vehicles are used.

The table also illustrates that minimizing total environmental impacts can reduce emissions by more than 10 % and 70 %, respectively, compared to the results obtained in the first scenario when the objective is to minimize the total cost and total time. Therefore, it is significant to consider environmental impacts and reduce environmental emissions. Furthermore, comparing the number of vehicles required in different scenarios confirms the importance of using Type 2, Type 3, and Type 4 vehicles in the waste clean-up system.

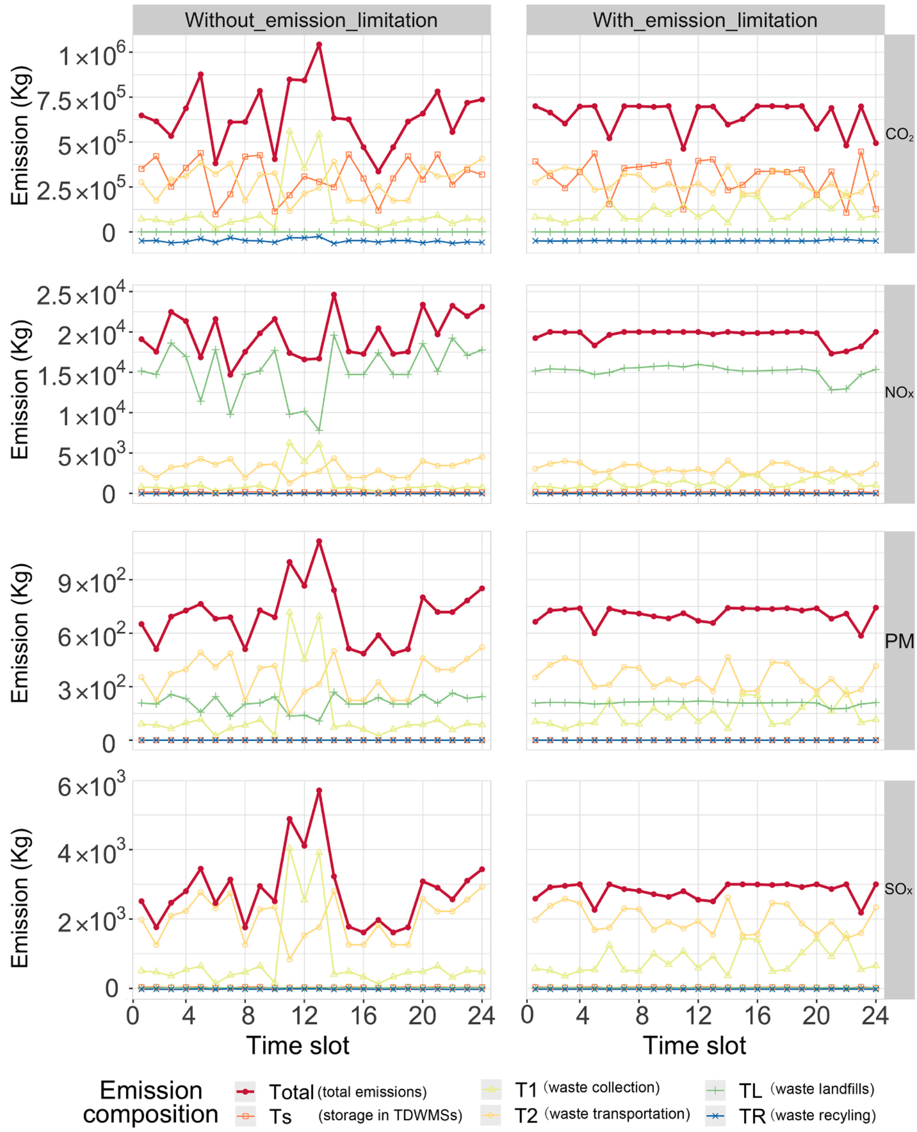

Fig. 7. Environmental emission composition in each time slot when minimizing total environmental impacts.

5.4. Cost and environmental emission analysis

Fig. 6 shows the amount and composition of the cost spent in each time slot when the objective is to minimize the total cost. The cost includes VOC, VOT, EC, SC, Operation and Storage Cost in TDWMSs (OSC), Landfill Cost (LC), and Recycling Cost (RC).

It shows that the cost spent in every time slot ranges between 2×10^6AUD to 8.5×10^6AUD with an average of around 5×10^6AUD. According to the definition of total cost presented in the model (Equation (35) to (38)), the cost of each time slot depends on the following factors: i) amount of waste transported between nodes in different stages; ii) distances of routes used in different stages; iii) amount of waste stored in the selected TDWMSs; iv) amount of waste sent to final disposal facilities. The first two factors determine the VOC, VOT, EC, and SC of vehicles used in each time slot, contributing to the total cost. The diversity of the combination of waste transportation amount and distance between nodes makes the cost distribution flux according to time, especially without daily cost constraints. The Figure also indicates that the RC can deduct about one-fourth of the total cost, emphasizing recycling in disaster waste management.

Fig. 7 presents the composition of *CO*2, *SOx*, *NOx*, and *PM* emissions on the left side when optimizing total environment impacts is the objective. The emissions come from waste collection (T1), waste transportation (T2), storage in TDWMSs (Ts), waste landfills (TL), and waste recycling (TR). The figures demonstrate that waste storage in TDWMSs and waste transportation are the most significant contributions to *CO*2 and the majority of *SOx* emission comes from waste transportation. The landfill has little impact on *CO*2 and *SOx* emissions. However, it takes a significant proportion of *NOx* and *PM* emissions. Furthermore, landfill contributes a dominant

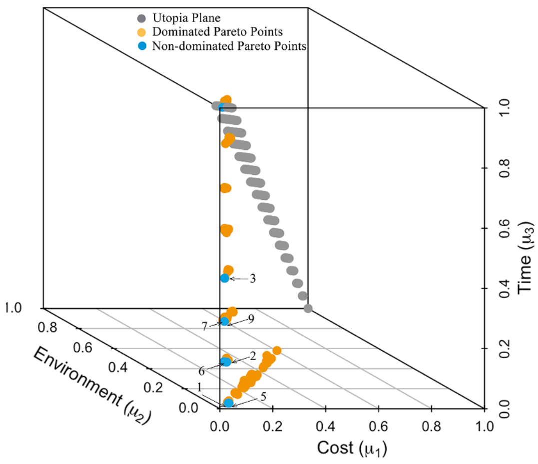

Fig. 8. Pareto frontier generated for the problem (m1 = 34).

proportion of *NOx* emission. In addition, landfill is the second most extensive resource of *PM* emission, following waste transportation.

According to figures on the left side of Fig. 7, the environmental emission fluctuates widely in different time slots and peaks in the time slot of 13. The reason could be attributed to the above reasons such as distance and amount. Specifically, at time slot 13, the amount of waste transported from the customer node to selected TDWMSs is high. The distance between the node pairs visited in time slot 13 is long in stage 1. It leads to a sizeable environmental emission in stage 1. However, in the actual waste clean-up practice, the system design needs to consider environmental capacity, i.e., the limit to absorb pollution in a certain period. Therefore, controlling the peak of environmental emissions and evenly distributing them across each time slot is necessary. A set of constraints (6) below are then added to the model. Constraints (41) ensure that each type of emission cannot exceed the limitation of each time slot. The figures on the right side of Fig. 7 show the distribution of each factor with environmental capacity limitations. The environmental emissions in each time slot are evenly distributed, ensuring the environmental capacities are satisfied.

$$p_{\omega}^{\mathrm{CO2}} \leq 7 \times 10^5, \forall \omega \in W$$

$$p_{\omega}^{\mathrm{SO}x} \leq 3 \times 10^3, \forall \omega \in W$$

$$p_{\omega}^{\mathrm{NO}x} \leq 2 \times 10^4, \forall \omega \in W$$

$$p_{\omega}^{\mathrm{PM}} \leq 750, \forall \omega \in W \tag{41}$$

5.5. *Pareto frontier*

The Pareto frontier is generated using MATLAB 2018b within 2 s. The order of objectives considered in this section is objective 1 (minimizing the total cost, μ^1), objective 2 (minimizing total environmental emission, μ^2), and objective 3 (minimizing the total time, μ^3). Based on the results provided in section 5.1, the anchor points μ^i are:

$\mu^1 = [1.17 \times 10^8\ 1.76 \times 10^7\ 24]$.

$\mu^2 = [1.27 \times 10^8\ 1.60 \times 10^7\ 24]$.

$\mu^3 = [5.56 \times 10^8\ 4.96 \times 10^7\ 17]$ (42).

Then the normalized anchor points are calculated in Equation (43), and the direction vectors are presented in Equation (44).

$$\overline{u}^1 = [0 \quad 0.05 \quad 1]$$

$$\overline{u}^2 = [0.02 \quad 0 \quad 1]$$

$$\overline{u}^3 = [1 \quad 1 \quad 0] \tag{43}$$

$$\overline{N}_1 = [1 \quad 0.95 \quad -1]$$

$$\overline{N}_2 = [0.92 \quad 1 \quad -1] \tag{44}$$

Fig. 8 shows the result of the Pareto frontier constructed using the method proposed in Appendix A.2. In this Figure, the points indicate the best combinations of the objectives. Fig. 8 also illustrates that most of the points in the original Pareto frontier are dominated by others. Finally, 9 points are non-dominated. The reason is that the total cost and total environmental emissions strongly depend on the total travel distance of vehicles. Thus, the two objectives only have a weak conflict with each other.

Table 6
Objective values of non-dominated points.

Point	Total cost (AUD)	Total environmental emission (Kg)	Total time (time slots)
Point 1	1.47×10^8	1.79×10^7	17
Point 2	1.38×10^8	1.72×10^7	18
Point 3	1.28×10^8	1.66×10^7	20
Point 4	1.23×10^8	1.63×10^7	24
Point 5	1.48×10^8	1.78×10^7	17
Point 6	1.37×10^8	1.73×10^7	18
Point 7	1.28×10^8	1.67×10^7	19
Point 8	1.24×10^8	1.62×10^7	24
Point 9	1.30×10^8	1.66×10^7	19

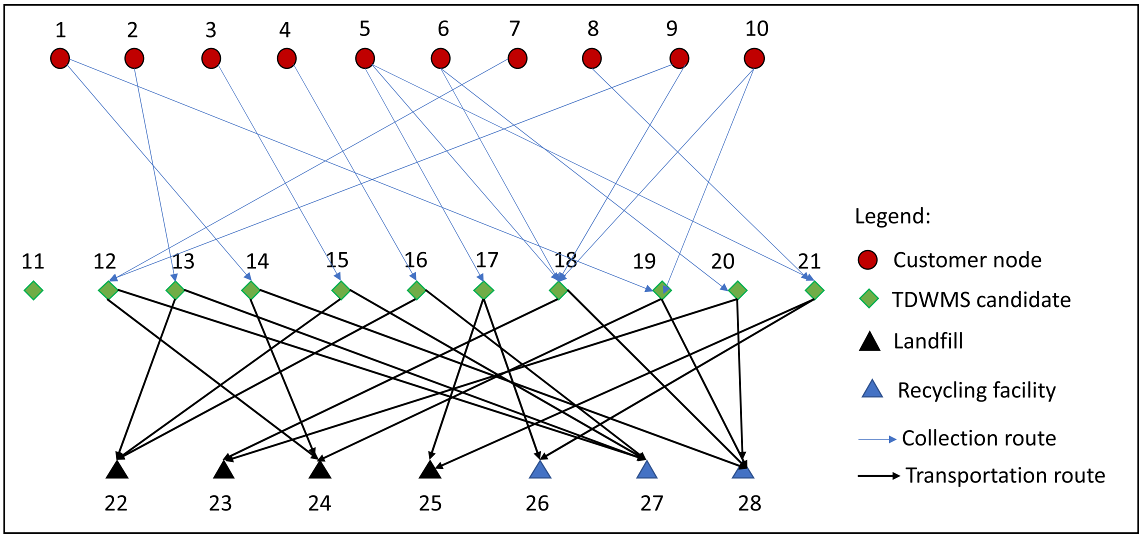

Fig. B1. Collection and transportation routes used in point 1 in Fig. 5.

Table B1
Waste flow of point 1.

From	To	Amount (ton)	From	To	Amount (ton)
1	14	18,227	14	24	9113
1	19	623,365	15	22	1033
2	13	9470	16	22	1340
3	15	2066	17	25	40,102
4	16	2680	18	23	47,009
5	17	80,204	19	24	335,992
5	18	15,857	20	23	278,076
5	21	8760	21	25	5447
6	18	25,500	12	27	17,480
6	20	556,152	13	27	4735
7	12	22,242	14	28	9113
8	21	2134	15	27	1033
9	12	12,717	16	27	1340
9	18	2648	17	26	40,102
10	18	50,012	18	28	47,009
10	19	48,619	19	28	335,992
12	24	17,480	20	28	278,076
13	22	4735	21	26	5447

In Table 6, we translate the non-dominated points to the actual value of each objective, which compromises the non-dominated results considering all objectives together. The decision-makers can select a waste clean-up plan according to their preference of the objectives. If the total cost and environmental emission are the main concerns, the results provided in Point 4 and Point 8 are good choices. If it is more important to recover the disaster-affected area as soon as possible, plans associated with Point 1 and Point 5 are better options. The results also generated transportation routes and waste flow in each point shown in Appendix B using point 1 as an example.

6. Conclusion remarks

6.1. Major findings

Integrating the location of processing facilities with vehicle transportation decisions is essential for establishing an efficient waste clean-up system, and the literature has dedicated much attention to the resulting optimization problems. However, few studies have proposed algorithms that simultaneously consider cost, time, and emissions outcomes across different waste removal arrangements, especially in the context of large scale. This study investigates how to achieve multiple-objective management in a two-echelon waste clean-up system that considers the location of TDWMS and truck fleet composition. A mixed-integer programming model in this study explicitly considers total operation time, cost, and environmental emissions. The most significant findings of this study can be summarized as follows:

i) The multiple objectives can be simultaneously considered by the mixed-integer programming model, which can be solved with black-box tools in very reasonable times. This time efficiency allows the model to be solved multiple times and their results applied to an NNCM to generate a Pareto frontier of the objectives. The computational efficiency of the approach allows for the methodology to be applied to large-scale decision problems.

ii) The three objectives related to time, cost and emissions are conflictive with each other. The solutions are analyzed from this perspective, and a series of managerial insights are obtained. For example, increased use of heavy-duty trucks can save about 50 % of the total cost and time but significantly increase environmental emissions.

iii) Minimizing the total environmental emissions can lead to an 87 % reduction of pollutants emissions. Considering environmental emission limitations in each time slot can help evenly release the pollutants to the environment without increasing the total amount.

6.2. Managerial implication

The model results can enable decision-makers to make efficient waste clean-up plans regarding selecting TDWMSs and vehicle fleets. It also helps design the transportation networks to and from the intermediate facilities. The availability of multiple non-dominated solutions can help decision-makers obtain ex-ante evaluations of a policy scheme.

Appropriate post-disaster waste management solutions can be formulated according to specific situations or requirements limiting emissions, time, or costs. The Pareto frontier analysis provides valid reference information for the decision-makers to allocate the funds and balance the environmental emission at each time slot. On the other hand, the numerical results can help convince stakeholders with different interests by justifying, for example, small losses in one of the objectives in the benefit of large gains in other aspects of the problem.

The analysis outcomes also indicate that solely pursuing one of the problem objectives can lead to serious drawbacks with respect to the solutions that explicitly consider all dimensions of the problem. In particular, it allows for conclusions regarding the importance of limiting carbon emissions.

6.3. Limitations and suggestions

Given the limited data, this paper did not integrate truck routing optimization in this model. We also do not consider the impacts of traffic on the route choice for waste collection and transportation, especially in areas close to urban developments. Finally, carbon emissions modeling can be improved with the use of real-time behavior models. These are interesting topics for future investigations.

Fund

This research was partially funded by the Australian Government through the Australian Research Council Industrial Transformation Training Centre in Optimisation Technologies, Integrated Methodologies, and Applications (OPTIMA), Project IDIC200100009; Global Environment Facility, Project P159883; Jiangsu Province Communications Department, Project 2018Y02_CFT/CS-6; and Shenzhen Municipal Natural Science Fund, Project JCYJ20190806144618382.

CRediT authorship contribution statement

Cheng Cheng: Conceptualization, Methodology, Software, Data curation, Writing – original draft, Writing – review & editing, Visualization. **Jia-Wei Lu:** Conceptualization, Writing – review & editing. **Rui Zhu:** Visualization, Writing – review & editing. **Zuopeng Xiao:** Writing – review & editing. **Alysson M. Costa:** Conceptualization, Methodology, Writing – review & editing. **Russell G. Thompson:** Supervision.

Declaration of Competing Interest

The authors declare that they have no known competing financial interests or personal relationships that could have appeared to influence the work reported in this paper.

Acknowledgement

We would like to thank the anonymous reviewers for taking the time and effort necessary to review the manuscript. We sincerely appreciate all valuable comments and suggestions, which helped us to improve the quality of the manuscript.

Appendix A:. The steps for Pareto frontier generation Pareto frontier

Step 1: Anchor Points generation. Anchor points are generated by sequentially considering each objective in the optimization model. The optimization model is run once for each objective, and the values obtained for all objectives for each run define the anchor points. The three anchor points define the utopia plane. In our case, we will get the following anchor points:

$\mu_1 = [\mathrm{objC_c\ objC_e\ objC_t}]$.

$\mu_2 = [\mathrm{objE_c\ objE_e\ objE_t}]$.

$\mu_3 = [\mathrm{objT_c\ objT_e\ objT_t}]$ (A1).

Step 2: Objectives normalisation. To avoid scaling deficiencies, the normalization of objectives is required to generate the Pareto frontier. To normalize the objectives, we defined the Utopia point in our case as $\mu_\mu = [objC_c\ objE_e\ objT_t]$. Based on the values of objectives obtained in step one, we can get the distance between the worst and best case of the objective values $L = [l_c\ l_e\ l_t]$.

$\mathrm{l_c = max(objE_c, objT_c) - objC_c}$.

$\mathrm{l_e = max(objC_e, objT_e) - objE_e}$.

$\mathrm{l_t = max(objC_t, objE_t) - objT_t}$ (A2).

Using the above definitions, the normalised design metrics can be evaluated as:

$$\overline{u}_1 = (\mu_1 - \mu_\mu)/L$$

$$\overline{u}_2 = (\mu_2 - \mu_\mu)/L$$

$$\overline{u}_3 = (\mu_3 - \mu_\mu)/L \tag{A3}$$

Step3: Computation of Utopia Plane Vectors. Utopia plane vector $\overline{N}_k$ defines the direction from $\overline{u}_n$ to $\overline{u}_k$. In our case, we have.

$$\overline{N}_1 = \overline{u}_3 - \overline{u}_2$$

$$\overline{N}_2 = \overline{u}_3 - \overline{u}_1 \tag{A4}$$

Step 4: Normalisation of Increments. The increment (δ_k) along the direction $\overline{N}_k$ are defined to decide the number of solutions (m_k) we want to obtain along with the associated $\overline{N}_k$ direction.

$\delta_k = 1/(m_k - 1)$ (A5).

To make sure points are evenly distributed on the utopia plane, we can use the following relationship. Given a specified number of points (m1) along the vector $\overline{N}_1$, we can set $\overline{N}_k$ as.

$m_k = m_1 |\ \overline{N}_k\ |/|\ \overline{N}_1\ |$ (A6).

Step 5: Utopia Plane Points generation. This step aims to evaluate a set of evenly distributed points on the utopia plane as:

$$\overline{X}_j = \sum_{k=1}^{3} a_{kj}\overline{u}_k \tag{A7}$$

Note that the value αkj should respect:

$$0 \le \alpha_{kj} \le 1. \tag{A8}$$

$$\sum_{k=1}^{3} a_{kj} = 1 \tag{A9}$$

The value of α_{kj} depends on the increments δ_k, which can be calculated using the Algorithm 1.

Algorithm 1. *α Generation.*

$j = 0$
$\alpha = 0$
while $\alpha \leq m_i$ **do**
  $j = j + 1$
  $\alpha_{1j} = \alpha * \delta 1$
  $\alpha_{2j} = 0$
  $\alpha_{3j} = 1 - \alpha_{1j}$
  while $\alpha_{1j} + \alpha_{2j} + \delta_2 <= 1$ **do**
    $j = j + 1$
    $\alpha_{1j} = \alpha_{1j} - 1$
    $\alpha_{2j} = \alpha_{2j} - 1 + \delta_2$
    $\alpha_{3j} = 1\text{-}\alpha_{1j} - \alpha_{2j}$
  end
end
return α

Step 6: Pareto Points generation. To generate Pareto points, we run the optimisation for J times by minimizing the total time objective considering the additional constraints in the following for each run *j*.

$$\overline{N}_k u - \overline{X}_j^T \leqslant 0 \quad 10)$$

$$\overline{u} = \{ \overline{u}_1 \quad \overline{u}_2 \quad \overline{u}_3 \} \quad 11)$$

Step 7: Generate Non-dominated Pareto Frontiers. In the final step, we applied the Pareto filter presented by Messac et al. (2003) to produce a subset of the Pareto points generated in Step 6 for which none will be dominated by any other. The filter aims to eliminate all dominated points from the Pareto frontier.

Appendix B:

Refer Fig. B1 and Table B1.

References

Alziari, S., Stepien, G., Durand, R., 1981. In vitro incorporation of (35S)-methionine in mitochondrial proteins of drosophila melanogaster. Biochem. Biophys. Res. Commun. 99, 1–8.
Amato, A., Gabrielli, F., Spinozzi, F., Magi Galluzzi, L., Balducci, S., Beolchini, F., 2019. Strategies of disaster waste management after an earthquake: A sustainability assessment. Resour Conserv Recycl. 146, 590–597.
Amato, A., Gabrielli, F., Spinozzi, F., Magi Galluzzi, L., Balducci, S., Beolchini, F., 2020. Disaster waste management after flood events. J. Flood Risk Manag. 13, 1–9.
Asai, S., Akiyama, T., Tanouchi, H., Egusa, N., 2021. A numerical simulation of disaster waste disposal in Wakayama city by using DHT model. Int. J. GEOMATE. 20, 23–28.
Baycan, F., 2004. Emergency planning for disaster waste: A proposal based on the experience of the marmara earthquake in turkey. In: 2004 International Conference and Student Competition on post-disaster reconstruction "Planning for reconstruction" Coventry, UK, April 22–23, 2004.
Berktaş, N., Kara, B., Karaşan, O., 2016. Solution methodologies for debris removal in disaster response. EURO J. Comput. Optim. 4 (3–4), 403–445.
Brown, C., Milke, M., Seville, E., 2010. Disaster waste management case study: 2009 Victorian bushfires, Australia. Resilient Organisations Research Report. https://www.resorgs.org.nz/publications/disaster-waste-management-case-study-2009-victorian-bushfires-australia-2/.
Brown, C., Milke, M., Seville, E., 2011a. Disaster waste management: A review article. Waste Manage. 31, 1085–1098.
Brown, C., Milke, M., Seville, E., et al., 2011b. Disaster waste management following the 2009 Victorian bushfires. Aust. J. Emerg. Manag. 26, 17.
Brown, C., Milke, M., 2016. Recycling disaster waste: Feasibility, method and effectiveness. Resour. Conserv. Recycl. 106, 21–32.
Çelik, M., Ergun, Ö., Keskinocak, P., 2015. The post-disaster debris clearance problem under incomplete information. Oper Res. 63, 65–85.
Cheng, C., Thompson, R.G., 2016. Application of boolean logic and gis for determining suitable locations for temporary disaster waste management sites. Int. J. Disaster Risk Reduct. 20, 78–92.
Cheng, C., Zhu, R., Costa, A., Thompson, R., 2021a. Optimisation of waste clean-up after large-scale disasters. Waste Manage. 119, 1–10.
Cheng, C., Zhu, R., Costa, A.M., Thompson, R.G., Huang, X., 2021b. Multi-period two-echelon location routing problem for disaster waste clean-up. TRANSPORTMETRICA A. https://doi.org/10.1080/23249935.2021.1916644.
County of San Diego, 2005. County of San Diego debris removal and recycling programs for the 2003 Cedar & Paradise fires final report. Report.
EPA, 2016. Waste Transfer Stations: A Manual for Decision-Making. https://www.epa.gov/sites/default/files/2016-03/documents/r02002.pdf.
FEMA, 2007. US FEMA(2007) Public assistance: debris management guide. [Washington, DC] : US Dept. of Homeland Security, Federal Emergency Management Agency, [2007].
Fetter, G., Rakes, T., 2012. Incorporating recycling into post-disaster debris disposal. Socio-Econ. Plan. Sci. 46, 14–22.
Habib, M., Sarkar, B., Tayyab, M., Saleem, M., Hussain, A., Ullah, M., Omair, M., Iqbal, M., 2019. Large-scale disaster waste management under uncertain environment. J. Clean. Prod. 212, 200–222.
Hu, Z., Sheu, J., 2013. Post-disaster debris reverses logistics management under psychological cost minimization. TRANSPORT RES B-METH. 55, 118–141.
Hu, Z., Sheu, J., Wei, C., Hu, S., 2019. Post-storm debris removal considering traffic and psychological impacts. TRANSPORTMETRICA A. 15, 1145–1174.
Karunasena, G., Amaratunga, D., Haigh, R., 2012. Post-disaster construction & demolition debris management: a Sri Lanka case study. J. Civ. Eng. Manag. 18, 457–468.
Kim, J., Deshmukh, A., Hastak, M., 2014. Selecting a temporary debris management site for effective debris removal. In: The 10th International Conference of the International Institute for Infrastructure Resilience and Reconstruction (I3R2) 20–22, May 2014, West Lafayette, Indiana, USA.
Lorca, A., Celik, M., Ergun, O., Keskinocak, P., 2017. An optimization-based decision-support tool for post-disaster debris operations. Prod Oper Manag. 26, 1076–1091.

Lu, J.W., Chang, N.B., Liao, L., Liao, M.Y., 2015. Smart and green urban solid waste collection systems: advances, challenges, and perspectives. IEEE Syst J. 11, 2804–2817.
Mamashli, Z., Nayeri, S., Tavakkoli-Moghaddam, R., Sazvar, Z., Javadian, N., 2021. Designing a sustainable-resilient disaster waste management system under hybrid uncertainty: A case study. Eng Appl Artif Intell. 106, 10445.
Messac, A., Ismail-Yahaya, A., Mattson, C.A., 2003. The normalized normal constraint method for generating the Pareto frontier. Struct Multidiscipl Optim. 25, 86–98.
Oh, G., Kang, Y., 2013. The status of flood wastes treatment and future tasks in South Korea. J. Mater. Cycles Waste Manag. 15, 282–289.
Onan, K., Ülengin, F., Sennaroğlu, B., 2015. An evolutionary multi-objective optimization approach to disaster waste management: A case study of Istanbul, turkey. Expert Syst. Appl. 42, 8850–8857.
Özdamar, L., Aksu, D.T., Ergüneş, B., 2014. Coordinating debris clean-up operations in post-disaster road networks. Socio-Econ. Plan. Sci. 48, 249–262.
Pramudita, A., Taniguchi, E., Qureshi, A.G., 2014. Location and routing problems of debris collection operation after disasters with realistic case study. Procedia Soc Behav Sci. 125, 445–458.
Qiu, Y., Zhou, D., Du, Y., Liu, J., Pardalos, P.M., Qiao, J., 2021. The two-echelon production routing problem with cross-docking satellites. TRANSPORT RES E-LOG. 147, 102210.
Rafee, N., Karbassi, A.R., Nouri, J., Safari, E., Mehrdadi, M., 2008. Strategic Management of Municipal Debris aftermath of an earthquake. Int. J. Environ. Res. 2, 205–214.
Rawtec, 2015. Disaster waste management scoping study. Technical Report. Office of Green Industries, South Australia, Australia.
Sahin, H., Kara, B., Karasan, O., 2016. Debris removal during disaster response: A case for turkey. Socio-Econ. Plan. Sci. 53, 49–59.
Sanchis, J., Martinez, M., Blasco, X., Salcedo, J., 2008. A new perspective on multi-objective optimization by enhanced normalized normal constraint method. Struct Multidiscipl Optim. 36, 537–546.
Sheu, J., 2007. A coordinated reverse logistics system for regional management of multi-source hazardous wastes. Comput Oper Res. 34, 1442–1462.
Syrichas, A., Crispin, A., 2017. Large-scale vehicle routing problems: Quantum annealing, tunings and results. Comput Oper Res. 87, 52–62.
Tabata, T., Wakabayashi, Y., Tsai, P., Saeki, T., 2017. Environmental and economic evaluation of pre-disaster plans for disaster waste management: Case study of minami-ise. Japan. Waste Manage. 61, 386–396.
Takeda, T., Mori, Y., Kubota, N., Arai, Y., 2014. A route planning for disaster waste disposal based on robot technology. In: In: Robotic Intelligence In Informationally Structured Space (RiiSS), 2014 IEEE Symp. Robot. Intell. Informationally Struct. https://doi.org/10.1109/RIISS.2014.7009173.
Yang, Y., Perera, L., Thompson, R.G., 2016. Truck cost analysis. Technical Report. Infrastructure Engineering Department, University of Melbourne.
Zhang, F., Cao, C., Li, C., Liu, Y., Huisingh, D., 2019. A systematic review of recent developments in disaster waste management. J. Clean. Prod. 235, 822–840.
Zhong, S., Cheng, R., Jiang, Y., Wang, Z., Larsen, A., Nielsen, O.A., 2020. Risk-averse optimization of disaster relief facility location and vehicle routing under stochastic demand. TRANSPORT RES E-LOG. 141, 102015.